Attosecond Imaging of Electronic Wave Packets

Gabriel A. Stewart, Paul Hoerner, Duke A. Debrah, Suk Kyoung Lee, H. Bernhard Schlegel and Wen Li*

*wli@chem.wayne.edu

Department of Chemistry, Wayne State University, Detroit, MI, 48202, USA

Abstract: An electronic wave packet has significant spatial evolution besides its temporal evolution, due to the delocalized nature of composing electronic states. The spatial evolution was not previously accessible to experimental investigations at the attosecond time scale. A phase-resolved two-electron-angular-streaking (PR-2eAS) method was developed to image the shape of the hole density of an ultrafast spin-orbit wave packet in the krypton cation. Furthermore, the motion of an even faster wave packet in the xenon cation was captured for the first time: an electronic hole being re-filled 1.2 fs after it was produced, and the hole-filling was observed in the opposite side where the hole was born.

Electron motions underpin some of the most fundamental phenomena in chemistry, physics, and biology. How to capture the spatial evolution of electrons at their native time scale (attoseconds to a few femtoseconds) is a grand challenge. The ultrafast temporal evolution has been addressed over the past two decades by developing attosecond spectroscopy to produce and probe electronic wave packets with various techniques. These include XUV-pump–IR-probe[1,2], attosecond transient absorption spectroscopy[3-5] and high harmonic spectroscopy[6,7]. However, these techniques do not directly measure the spatial distributions/evolution of the electronic wave packets. This renders existing measurements one dimensional in nature while the spatial distribution/evolution must be inferred from theoretical calculations. Time-resolved imaging techniques do exist[8-10], but these are not operable at attoseconds to a few femtoseconds time scale.

Attosecond angular streaking, also known as attoclock, was first developed to measure ionization delays in single or double ionization[11-14]. It was recently developed into a pump-probe method[15,16] and captured ultrafast double ionization dynamics within the first femtosecond (2eAS)[17]. In this method, strong field ionization is utilized in both the pump and probe steps while the time delays are obtained from the relative ejection angles between the two ejected electrons in a circularly polarized strong field. The rotating electric field employed in the method offers a unique opportunity for spatial imaging of electronic orbitals because the angle dependent ionization rates can map out the shape of orbitals[18,19]. Here we show it has now become possible to combine the two features (attosecond time resolution and orbital mapping) and achieve attosecond imaging of the ultrafast spin-orbit wave packet motions in the xenon cation for the first time.

Strong field ionization of noble gas atoms produces a manifold of cation states with a hole in the outermost p orbitals[20]. The energies of those states are separated into the low ${}^{2}P_{3/2}$ and high ${}^{2}P_{1/2}$ states, with the splitting determined by the strength of spin-orbit interaction. The shapes (electron

density) of these states are different depending on their corresponding compositions of spatial orbitals (p_0 and $p_{\pm l}$). It has been shown that the produced cation states are coherent and therefore electronic wave packets with significant spatial evolution is expected[3,21,22]. We carried out simulations on ionizations of these cation wave packets by circularly polarized intense fields. The calculations are based on time-dependent configuration interaction calculations using a CISD-IP wavefunction that consists of singly ionized configurations and singly excited, singly ionized configurations (TD-CISD-IP)[23] (see Supplementary Material for detailed theoretical methodology, which include Refs. [24-42]). The results show that the angle dependent ionization rates can indeed map out the shape of electronic wave packet at different time delays (Fig. 1A) for both xenon and krypton: at time zero, the ionization rate suggests the hole shape looks like a peanut

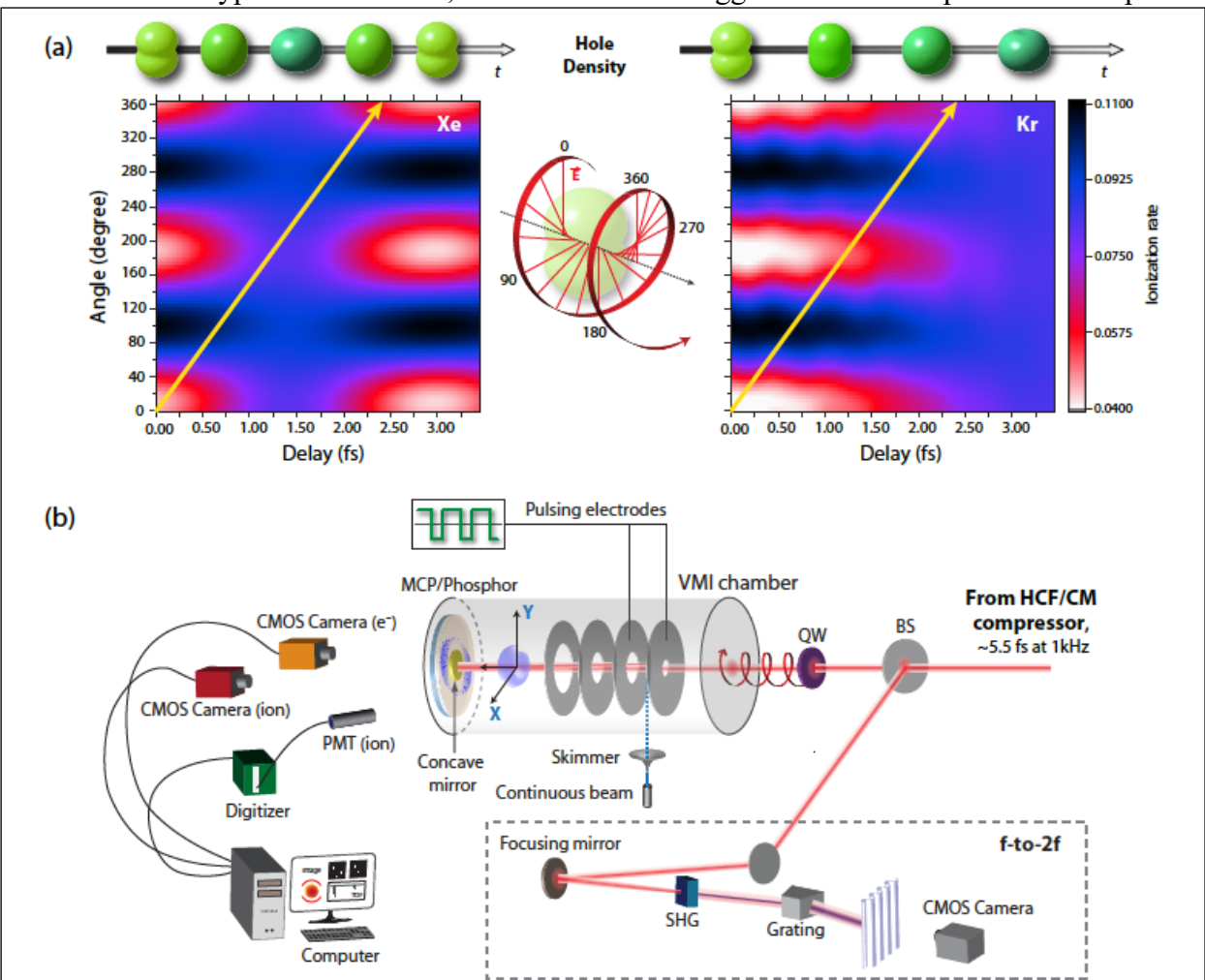


Figure 1 Attosecond imaging of electronic wave packets. (a) Top: the temporal evolution of electronic wave packets in the form of hole density in the xenon cation (left) and krypton cation (right). Bottom: the calculated time- and angle- dependent ionization rates of an electronic wave packet with an initial phase of 0 degree. The angle dependence arises from the shape of hole density. The yellow lines represent the rotating electric field probing at different directions and time delays. The inset between the two plots illustrates how the rotating electric field of circularly polarized light can map the shape of electron (hole) density. (b) The experimental set-up for achieving phase-resolved 2eAS.

while at half period of wave packet motion, the shape is much more spherical due to hole filling dynamics. When utilizing circularly polarized light to probe such dynamics, because the direction of the electric field vector is rotating (360 degrees/laser period), the probing site changes with time (see the yellow diagonal line in Fig. 1A bottom) and therefore spatial-temporal imaging can be achieved.

The wave packet dynamics in the krypton cations (a period of $\sim 6.3 \, fs$) have been detected in a pioneering experiment with attosecond transient absorption spectroscopy (ATAS)[3]. Surprisingly, despite very similar electronic structures, wave packet motions in the xenon cations $(5p^{-1})$ have evaded detection so far[4,5]. This is likely due to the extremely fast dynamics in the xenon cation (a period of $\sim 3 \, fs$). Ionizations at different moments during an ultrashort laser pulse prevents the build-up of coherence in an ensemble of atoms and molecules[21]. Here we show, with coincidence techniques, the two-electron-angular-streaking technique (2eAS) can probe electronic coherence at single atom/molecule level and thus circumvents the requirement of ensemble coherence. The calculated time-resolved double ionization yield shows a clear difference between xenon and krypton. The much faster dynamics in the xenon cations manifest in the much shallower valley at 1.2 fs compared to krypton. This is because at 1.2 fs, the hole is being filled in xenon while this is not the case in krypton (Fig. 2A). Can we observe this in experiment?

The phase-resolved 2eAS measurements were performed on a newly developed coincidence/covariance electron imaging setup, as shown in Figure 1B. The vacuum chamber and the pulsing ion/electron coincidence velocity map imaging (VMI) spectrometer are similar to that described previously[43,44]. However, the laser-detector configuration is different and will be briefly described here (Fig. 1B). The laser pulse was produced by broadening the output of a Ti:sapphire amplifier laser system (KMLabs, Red Dragon, 1 kHz, 1 mJ/pulse and 30 fs pulse duration) using an argon filled 1-m long hollow-core-fiber (Imperial Consultants (ICON) of Imperial College London). The beam was further compressed with 7 pairs of chirped mirrors (Ultrafast Innovation, PC70). The compressed pulses were fully characterized using a dispersion scan (d-scan) technique [45] to be ~5.5 fs in pulse width. The short pulse duration is essential because it restricts the double ionization within one laser cycle and removes time ambiguity associated with multi-cycle pulses and angular streaking. Using an ultrabroadband quarter-wave plate, close-to-circular polarized light was produced (ellipticity ~.93). This beam entered the vacuum chamber toward the MCP/phosphor imaging detector. Before reaching the detector, it was reflected by a 7.5 cm focal-length concave mirror and focused backward onto a continuous atomic/molecular gas jet to produce ions and electrons. Because the mirror was located at the fieldfree area of the VMI spectrometer, it did not cause significant field distortion. The laser intensity was ~2×10¹⁴ W/cm². The ions and electrons were accelerated and velocity-focused by a VMI spectrometer using pulsed high voltage on the repeller and the extractor. The two dimension hit positions of each ion and electron were recorded by two separate cameras, both of which were triggered by the laser at 1 kHz but their exposure time windows were adjusted to detect only ions or only electrons. The ion time-of-flight was obtained by picking off the MCP signal and digitizing it with a high-speed digitizer. The TOF and hit position provide full 3D momentum information of each ion[46,47]. For electrons, only 2D momentum were measured even though the technique is capable of 3D momentum measurement of two electrons in coincidence. Finally, a camerabased f-to-2f setup was used to tag the relative carrier-envelope-phase (CEP) of each laser

pulse[44,48]. Because our laser is not phase stabilized, the tagging is critical for measuring the insitu absolute CEP of the pulses.

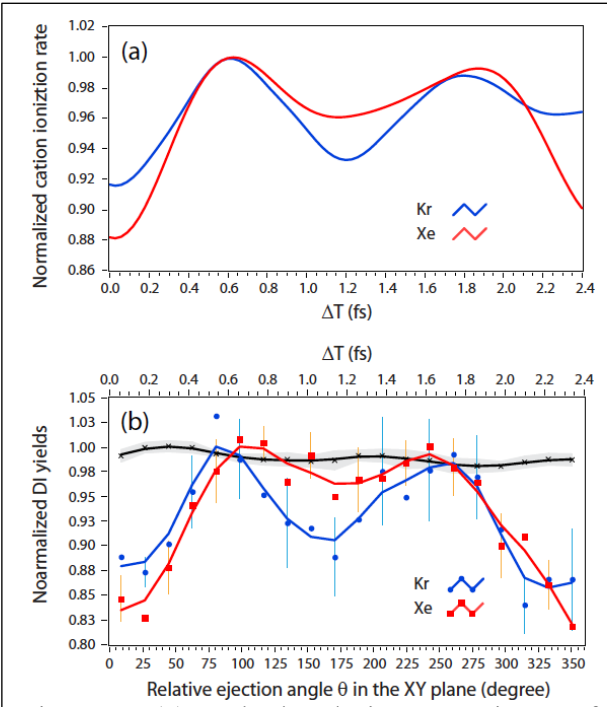


Figure 2 (a) Calculated time transients of second ionization yields of electronic wave packets in xenon and krypton cations as probed by a circularly polarized strong field, i.e., the ionization yields integrated along the yellow diagonal lines in Fig. 1A. Both were normalized to their corresponding maxima. (b) Experimentally obtained time transients of double ionization yields in xenon (red) and krypton (blue). The curves are the cubic spline fittings of the data points (blue round for krypton and red square for xenon). They were both normalized to their own maxima. The black curve and data points show the result of false coincidence events (two electrons plus a single cation), suggesting the system bias is minimum even with a high false coincidence rate. XY plane is the plane of polarization.

Two technical advancements implemented in this setup have enabled the phase-resolved angular streaking measurements: (1) employing a zero deadtime detection of two coincident electrons arising from double ionization, and (2) direct detection of the absolute carrierenvelope-phases (CEP) of few-cycle circularly polarized laser pulses. The first advancement utilized the special laser detector configuration with the 2D momentum of both electrons measured directly with a camera, which has no dead-time detecting two coincident electrons, superior to even the state-of-the-art 3D detectors in this case[46,49-51]. This allowed highly efficient detection of double ionization events and eliminated detection bias. An unusual coincidence scheme was also implemented to increase the effective count rate. An average count rate of 2 electrons/laser shot was used and only those events with exactly two electrons and one dication (xenon or krypton) were analyzed to extract the data. Due to the high event rate, false coincidence rate was high. However, because the false coincidence events had a flat relative angle vs. yield response (Fig. 2B black curve), they did not distort the true coincidence results other than reducing the modulation depth. On the other hand, this significantly boosted the data rate and made the current measurement possible. The false coincidence data also suggests the bias introduced by the non-perfect ellipticity (0.93) was minimum.

The second technical advancement solves a critical issue associated with the angular steaking technique: how to identify which electron is from the first ionization (neutral ionization) or the second ionization (cation

ionization). Because 2eAS is a single beam double ionization experiment, the time delays between the two ionization events are extracted from the ejection angle between the two electrons. Correctly identifying which electron is ionized first is critical to obtain the correct time delays. Previously, this was done by assigning the slower electron to be the first due to a lower laser intensity at the first ionization[13]. We first applied this method to retrieve the time dependent trace and the result

is shown in Fig. 2B, which shows a reasonable agreement with the theoretical prediction. This seems to suggest the method has correctly captured the main difference between the xenon and krypton. However, the similar yields between the early time delay around 0 fs (0 degree) and 2.4 fs (360 degree) is a suspect. This is because, when the second ionization is pinned around the peak of the laser envelope due to a much higher ionization potential, a longer time delay (e. g. ~2.4 fs vs. ~0 fs) between the first and second ionization means the neutral ionization takes place at the earlier leading edge of the pulse envelope, which has a lower intensity. This suggests that at a longer time delay, the yield should be reduced because of the lower intensity. The data in Fig. 2B do not show this trend. This failure is likely due to a significant transverse velocity distribution at the tunneling exit that prevents correct association[52] (see more details in Supplementary Material). One complication to this conclusion is when there is neutral depletion, and we will come back to this later.

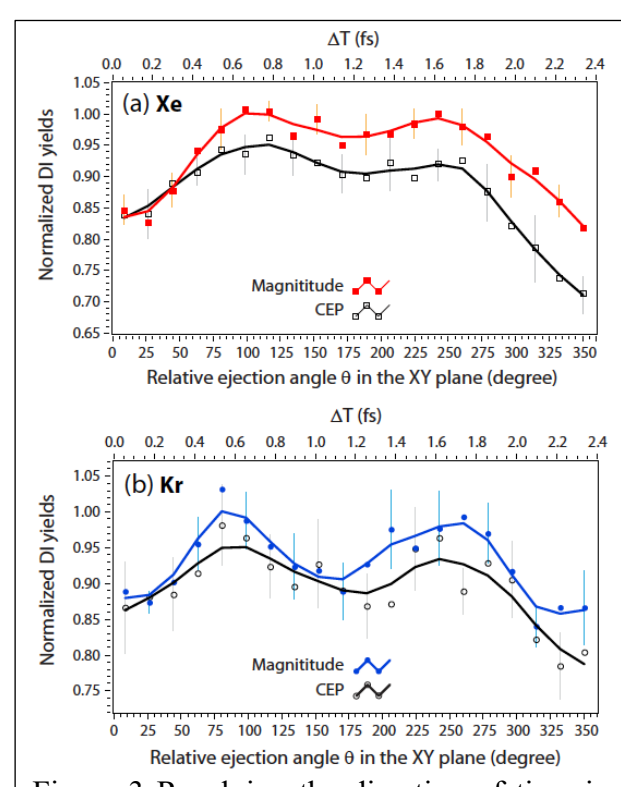


Figure 3 Resolving the direction of time in 2eAS with absolute CEP measurements in (a) xenon and (b) krypton. Comparison between time transients obtained with employing momentum magnitude or absolute CEP as the discriminators.

A phase-resolved angular streaking method is developed here to resolve this by exploiting the fact that the absolute CEP of circularly polarized light coincides with the peak of the laser envelope of few-cycle pulses. Because the second ionization is likely to occur around the peak of the laser envelope, the electron with an eiection direction closer to the corresponding to the absolute CEP should be the second electron (see Supplementary Material for verification). Such a measurement has not been possible until recently. A direct, insitu measurement of the absolute CEP of circularly polarized light was achieved[44,53] and it was employed here. The ejection angle associated with the absolute CEP determined to be along the direction which has the highest ionization yield for all the laser pulses having the same relative CEP, which was measured with the f-to-2f setup. We note, even though the second ionization most likely takes place at the peak of the laser envelope, our analysis does not impose such a restriction because picking which is the second electron does not alter the ejection angle of either electron. The new time (angle)- resolved double ionization yield was plotted in Fig. 3. The new result indeed shows a decrease of double

ionization yield toward longer (higher) time delays (angles). This trend is expected and validates the new approach for distinguishing the two electrons.

To further correct the laser envelope induced bias and reveal true time-resolved dynamics, the ionization probability of the neutral species before the envelope peak was calculated using

nonadiabatic tunneling theory[54] (See details in Supplementary Material). The results suggest neutral ionization was saturated ~1.6 fs before the peak due to the high laser intensity employed in the study. The insets in Fig. 4 shows the employed correction curves which is the inverse of the sum of time dependent ionization probability and a constant background signal accounting for the false coincidence events. The fully corrected time transients are shown in Figure 4. The excellent agreement between theory and experiment shows the new method has correctly captured the physics involved in the complex double ionization process and this enables the technique to time-resolve the ultrafast electronic wave packet motion.

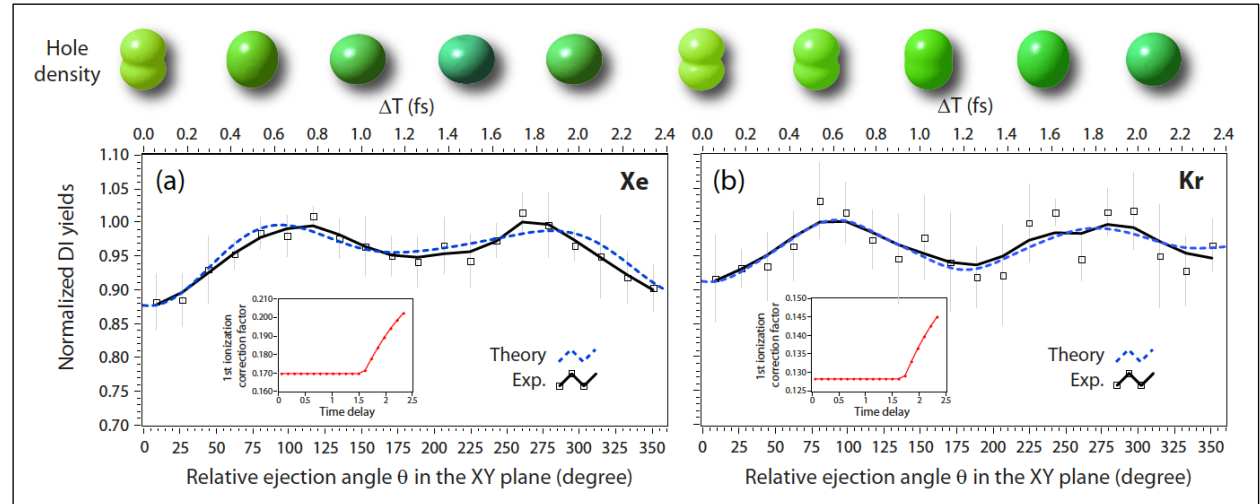


Figure 4 Fully corrected time transients showing the time-resolved double ionization yields, reflecting the spatio-temporal evolution of electronic wave packets in (a) xenon and (b) krypton. The insets show the time dependent functions used to correct the enveloped induced first ionization bias. The curves are the inverse of the sum between ionization probabilities of neutral xenon and krypton and time independent background signals arising from false coincidence events.

Now since we have established the validity of the new method, we can investigate the detailed strong field ionization dynamics revealed by the experiment. One important parameter of a wave packet is the initial phase between the states, which dictates the initial shape of the wave packet and its time evolution. In our measurement, a suppression of double ionization yield at time zero was observed in both xenon and krypton. This gave a 0 degree (±15°) of initial phase between the two states immediately after the tunneling ionization, confirming an initial peanut shaped hole. This initial phase has not been directly measured in previous studies either in krypton or xenon. In krypton, this shape remains for the first 1.2 fs (half of the laser period) and was clearly mapped out by the time- and angle- dependent double ionization yields. The slight signal change between 0 fs and 1.2 fs confirms this is a wave packet instead of a static eigen state. This is the first time that the shape of the hole density was directly mapped for the krypton cation. A 0 degree of initial phase was also obtained for the xenon cation. However, due to the much faster dynamics, the valley at 180 degrees is quickly filled at \sim 1.2 fs, leading to the observed time transients. From the best fitted theory results, the relative populations of ${}^{2}P_{3/2}$ and ${}^{2}P_{1/2}$ can be extracted to be about 0.75:0.25 for both xenon and krypton (See Supplementary Material for details). We should note the double ionization yield peaks in xenon deviate somewhat from the theoretical results. This is

likely due to different deflection angles for the first and second ionization of xenon, which were not modeled in our theoretical methods. The observed discrepancy can provide important clues on whether such a deflection angle change is due to tunneling time or non-adiabatic dynamics[55-57] and requires further investigations.

Acknowledgement

Research supported by the U.S. Department of Energy (DOE), Office of Science, Basic Energy Sciences (BES), under Award # DE-SC0020994 (Attosecond dynamics probed with angular streaking) and National Science Foundation (NSF), AMO-E program, under Award #2012098 (Absolute phase measurement).

- [1] F. Calegari *et al.*, Science **346**, 336 (2014).
- [2] M. Lara-Astiaso *et al.*, J. Phys. Chem. Lett. **9**, 4570 (2018).
- [3] E. Goulielmakis et al., Nature **466**, 739 (2010).
- [4] Y. Kobayashi, M. Reduzzi, K. F. Chang, H. Timmers, D. M. Neumark, and S. R. Leone, Phys. Rev. Lett. **120**, 233201 (2018).
- [5] M. Sabbar, H. Timmers, Y.-J. Chen, A. K. Pymer, Z.-H. Loh, Scott G. Sayres, S. Pabst, R. Santra, and S. R. Leone, Nat. Phys. **13**, 472 (2017).
- [6] O. Smirnova, Y. Mairesse, S. Patchkovskii, N. Dudovich, D. Villeneuve, P. Corkum, and M. Y. Ivanov, Nature **460**, 972 (2009).
- [7] P. M. Kraus *et al.*, Science **350**, 790 (2015).
- [8] M. Kübel, Z. Dube, A. Y. Naumov, D. M. Villeneuve, P. B. Corkum, and A. Staudte, Nat. Commun. 10, 1042 (2019).
- [9] W. Li, A. A. Jaron-Becker, C. W. Hogle, V. Sharma, X. Zhou, A. Becker, H. C. Kapteyn, and M. M. Murnane, Proc. Natl. Acad. Sci. U. S. A. **107**, 20219 (2010).
- [10] A. Fleischer et al., Phys. Rev. Lett. **107**, 113003 (2011).
- [11] P. Eckle, A. N. Pfeiffer, C. Cirelli, A. Staudte, R. Dörner, H. G. Muller, M. Büttiker, and U. Keller, Science **322**, 1525 (2008).
- [12] P. Eckle, M. Smolarski, P. Schlup, J. Biegert, A. Staudte, M. Schoffler, H. G. Muller, R. Dorner, and U. Keller, Nat. Phys. **4**, 565 (2008).
- [13] A. N. Pfeiffer, C. Cirelli, M. Smolarski, R. Dorner, and U. Keller, Nat. Phys. 7, 428 (2011).
- [14] A. N. Pfeiffer, C. Cirelli, M. Smolarski, X. Wang, J. H. Eberly, R. Doerner, and U. Keller, New J. Phys. **13**, 093008 (2011).
- [15] V. Hanus *et al.*, Phys. Rev. Lett. **123**, 263201 (2019).
- [16] V. Hanus et al., Phys. Rev. Lett. **124**, 103201 (2020).
- [17] A. H. Winney, S. K. Lee, Y. F. Lin, Q. Liao, P. Adhikari, G. Basnayake, H. B. Schlegel, and W. Li, Phys. Rev. Lett. **119**, 123201 (2017).
- [18] H. Akagi, T. Otobe, A. Staudte, A. Shiner, F. Turner, R. Dörner, D. M. Villeneuve, and P. B. Corkum, Science **325**, 1364 (2009).
- [19] A. H. Winney, G. Basnayake, D. A. Debrah, Y. F. Lin, S. K. Lee, P. Hoerner, Q. Liao, H. B. Schlegel, and W. Li, J. Phys. Chem. Lett. **9**, 2539 (2018).
- [20] L. Young et al., Phys. Rev. Lett. 97, 083601 (2006).

- [21] N. Rohringer and R. Santra, Phys. Rev. A **79**, 053402 (2009).
- [22] I. Barth and O. Smirnova, J. Phys. B-At. Mol. Opt. Phys. 47, 204020 (2014).
- [23] M. K. Lee, W. Li, and H. B. Schlegel, J. Chem. Phys. **152**, 064106 (2020).
- [24] T. H. Dunning, J. Chem. Phys. **90**, 1007 (1989).
- [25] M. J. Frisch, G. W. Trucks, H. B. Schlegel, G. E. Scuseria, and e. al., Gaussian Development Version, Gaussian, Inc., 2010.
- [26] A. A. Golubeva, P. A. Pieniazek, and A. I. Krylov, J. Chem. Phys. **130**, 124113 (2009).
- [27] P. Hoerner, M. K. Lee, and H. B. Schlegel, J. Chem. Phys. **151**, 054102 (2019).
- [28] P. Hoerner, W. Li, and H. B. Schlegel, J. Phys. Chem. A **124**, 4777 (2020).
- [29] P. Hoerner, W. Li, and H. B. Schlegel, J. Chem. Phys. **155**, 114103 (2021).
- [30] P. Hoerner and H. B. Schlegel, J. Phys. Chem. A **121**, 5940 (2017).
- [31] P. Hoerner and H. B. Schlegel, J. Phys. Chem. A **121**, 1336 (2017).
- [32] P. Hoerner and H. B. Schlegel, J. Phys. Chem. C **122**, 13751 (2018).
- [33] C. Huber and T. Klamroth, J. Chem. Phys. **134**, 054113 (2011).
- [34] P. Krause and H. B. Schlegel, J. Phys. Chem. Lett. **6**, 2140 (2015).
- [35] P. Krause and H. B. Schlegel, J. Phys. Chem. A **119**, 10212 (2015).
- [36] P. Krause, J. A. Sonk, and H. B. Schlegel, J. Chem. Phys. **140**, 174113 (2014).
- [37] M. K. Lee, P. Hoerner, W. Li, and H. B. Schlegel, J. Chem. Phys. **153**, 244109 (2020).
- [38] C. M. Marian, Wiley Interdiscip. Rev.: Comput. Mol. Sci. 2, 187 (2012).
- [39] K. A. Peterson, D. Figgen, E. Goll, H. Stoll, and M. Dolg, J. Chem. Phys. **119**, 11113 (2003).
- [40] K. A. Peterson, B. C. Shepler, D. Figgen, and H. Stoll, J. Phys. Chem. A **110**, 13877 (2006).
- [41] H. B. Schlegel, P. Hoerner, and W. Li, Front. Chem. **10**, 866137 (2022).
- [42] D. E. Woon and T. H. Dunning, J. Chem. Phys. **98**, 1358 (1993).
- [43] L. Fan et al., J. Chem. Phys. **147**, 013920 (2017).
- [44] D. A. Debrah, G. A. Stewart, G. Basnayake, J. W. G. Tisch, S. K. Lee, and W. Li, Opt. Lett. **44**, 3582 (2019).
- [45] M. Miranda, C. L. Arnold, T. Fordell, F. Silva, B. Alonso, R. Weigand, A. L'Huillier, and H. Crespo, Opt. Express **20**, 18732 (2012).
- [46] S. K. Lee, F. Cudry, Y. F. Lin, S. Lingenfelter, A. H. Winney, L. Fan, and W. Li, Rev. Sci. Instrum. **85**, 123303 (2014).
- [47] G. Basnayake, Y. Ranathunga, S. K. Lee, and W. Li, J. Phys. B-At. Mol. Opt. Phys. **55**, 023001 (2022).
- [48] X. Ren et al., J. Opt. 19, 124017 (2017).
- [49] S. K. Lee, Y. F. Lin, S. Lingenfelter, L. Fan, A. H. Winney, and W. Li, J. Chem. Phys. **141**, 221101 (2014).
- [50] Y. F. Lin, S. K. Lee, P. Adhikari, T. Herath, S. Lingenfelter, A. H. Winney, and W. Li, Rev. Sci. Instrum. **86**, 096110 (2015).
- [51] Q. Liao, A. H. Winney, S. K. Lee, Y. F. Lin, P. Adhikari, and W. Li, Phys. Rev. A **96**, 023401 (2017).
- [52] N. B. Delone and V. P. Krainov, J. Opt. Soc. Am. B: Opt. Phys. **8**, 1207 (1991).
- [53] S. Fukahori, T. Ando, S. Miura, R. Kanya, K. Yamanouchi, T. Rathje, and G. G. Paulus, Phys. Rev. A **95**, 053410 (2017).
- [54] G. L. Yudin and M. Y. Ivanov, Phys. Rev. A **64**, 013409 (2001).
- [55] L. Torlina et al., Nat. Phys. 11, 503 (2015).

- [56] A. S. Landsman, M. Weger, J. Maurer, R. Boge, A. Ludwig, S. Heuser, C. Cirelli, L. Gallmann, and U. Keller, Optica 1, 343 (2014).
- [57] N. Camus et al., Phys. Rev. Lett. **119**, 023201 (2017).